Submitted to The Astrophysical Journal
Preprint typeset using LaTeX style emulateapj v. 12/16/11

NOT SO HEAVY METALS: BLACK HOLE FEEDBACK ENRICHES THE CIRCUMGALACTIC MEDIUM

N. Nicole Sanchez[1], Jess Werk[1], Michael Tremmel[2], Andrew Pontzen[3], Charlotte Christensen[4], Tom Quinn[1], Akaxia Cruz[1], and [**Order subject to change**]

[1]Astronomy Department, University of Washington, Seattle, WA 98195, US, sanchenn@uw.edu
[2]Yale Center for Astronomy & Astrophysics, Physics Department, P.O. Box 208120, New Haven, CT 06520, USA
[3]Department of Physics & Astronomy, University College London, 132 Hampstead Road, London, NWI 2PS, United Kingdom and
[4]Physics Department, Grinnell College, 1116 Eighth Ave., Grinnell, IA 50112, United States

Submitted to The Astrophysical Journal

ABSTRACT

By tracing the redistribution of metals in the circumgalactic medium (CGM) via outflows, we show that Ovi is a sensitive indicator of supermassive black hole (SMBH) feedback. We examine the effects of SMBH feedback on the CGM using a cosmological hydrodynamic simulation (Romulus25 Tremmel et al. 2017) and a set of zoom-in "genetically modified" Milky Way-mass galaxies sampling different evolutionary paths. We compare the column densities of Ovi in Milky Way-mass galaxies and compare them with observations from the COS-Halos Survey; contrary to previous simulations which underpredicted the CGM column densities of Ovi, these simulations are consistent with COS-Halos observations *of star forming galaxies and slightly overpredict Ovi in quenched galaxies*. We determine that a galaxy's star formation history and accretion rate have little effect on the appearance of Ovi in its CGM while column densities of Ovi are more closely tied to galaxy halo mass. The set of zoom-in, genetically modified Milky Way-mass galaxies confirm that the SMBH acts as the physical mechanism for transporting metals out into its host halo thereby significantly impacting the appearance of Ovi found in the CGM.

Subject headings: Gas physics – Galaxies: circumgalactic medium – Galaxies: spiral – Galaxies: kinematics and dynamics – Methods: Numerical

1. INTRODUCTION

The circumgalactic medium (CGM), the extended region of gas surrounding galaxies out to their virial radii, is richly structured with the by-products of galaxy evolution. Due to its diffuse nature, the CGM remains one of the most difficult regions to observe. Beginning in 2010, observations of the CGM became possible due to technological advances like the Cosmic Origins Spectrograph (COS) on the Hubble Space Telescope (HST). Most observations have focused on UV and optical lines, using a variety of methods in addition to the absorption-line studies of COS-Halos, which use the light of a distant quasar to observe the absorption lines of CGM gas within galaxies in the line of sight. These methods include: stacking analyses, which combines hundreds or thousands of spectra to parse out the faint signals of CGM lines (York et al. 2006, Peek, Ménard and Corrales 2015, Steidel et al. 2010); "down-the-barrel" spectroscopy, which employs a galaxy's own starlight as the background source for CGM absorption (Martin 2005, Bordoloi et al. 2011, Rubin et al. 2014, Heckman et al. 2015); and emission line maps, which search for the few photons emitted directly by CGM gas (Putman, Peek and Joung 2012b, Hayes et al. 2016). The latter of these is also observed in X-ray, and additional X-ray observations by Chandra and XXM have also been used to help constrain the extent of the CGM (Nicastro et al. 2005)). Through these studies, observers have found the CGM region to be a structurally complex, multiphase medium (Tumlinson et al. 2011; Werk et al. 2012, 2013, 2016; Tumlinson et al. 2017). Studies like Werk et al. (2014) show that most of the "missing baryons" of galaxies likely reside in this diffuse region, implying that the CGM may play a key role in the growth of galaxies and the build up of their disks. Therefore, it is clear that understanding the CGM is crucial for understanding the complex nature of galaxy evolution and growth.

COS-Halos finds a correlation between the column densities of Ovi out to 150 kpc and the specific star formation rate (sSFR) of their observed galaxies. Higher column densities of Ovi are found around SF galaxies compared to their passive counterparts. Oppenheimer et al. (2016) argue that this bimodality arises due to the Ovi acting as a proxy for the virial temperature of gas in these galaxy halos. Therefore, more massive galaxies have more of their oxygen in a phase traced by Ovii and Oviii; thus, the COS-Halos sample show less Ovi in their CGM due to the intrinsically higher virial temperature of these massive red ellipticals. In contrast, Suresh et al. (2017) argue that the Ovi is built up by SMBH feedback, which can physically modify the CGM via outflows or heat it to the appropriate temperature for ionizing Ovi. In both cases, each argument implies an intrinsic link between the CGM and its host galaxy's evolution.

Additionally, galaxy evolution has been shown to be strongly tied to the evolution of its central supermassive black hole (SMBH). Through relations like the M-σ and the bulge mass-BH mass correlation (Ferrarese & Merritt 2000; Mcconnell & Ma 2013), recent studies indicate that the SMBH and its host galaxy halo *co-evolve* (Gebhardt et al. 2000; Volonteri & Bellovary 2012; Kormendy & Ho 2013; Reines & Volonteri 2015, and references therein). It is therefore unsurprising that a SMBH is thought to leave its marks on the CGM. However, the direct mechanisms by which the SMBH impacts the CGM are still debated.

SMBHs may effect the CGM in a variety of ways. First,

feedback from the active SMBH may inject energy into the surrounding material, raising temperatures, and ionizing metals in the gas [Cite]. Additionally, massive outflows of gas from the SMBH may physically push gas out of the galaxy [Cite]. Some of this gas may end up falling back into the galaxy as part of the "recycling" of the CGM (Tumlinson et al. 2017), enriching CGM gas with metals from the center of the galaxy, and further enriching the IGM as gas is expelled from the galaxy halo.

Cosmological hydrodynamic simulations have become a powerful tool for examining the physics driving the multiphase nature of the CGM (Cen 2013; Ford et al. 2016a; Oppenheimer et al. 2016; Suresh et al. 2017; Nelson et al. 2018). Simulators have long been examining the underlying physics of SMBH activity in galaxies; however, recent studies have proven that the observed properties of the CGM are not easily matched and the underlying physics of this region is a fairly new field ripe for discovery. Most previous studies have underpredicted the column densities of Ovi found by COS-Halos (including the aforementioned studies Oppenheimer & Davé (2008) and Suresh et al. (2017)); however, important strides have started to be made in probing this diffuse region. Using the smooth particle hydrodynamic code GADGET-2 (Springel & Hernquist 2005; Oppenheimer & Davé 2008), Ford et al. (2016b) found that the presence of Ovi in the CGM likely arises from metals ejected early on in the galaxy's evolution. More recently, Nelson et al. (2018) well-matched the COS-Halos observations using the IllustrisTNG simulations and determined that the amount of Ovi the the CGM can depend on a variety of galactic properties including sSFR. In particular, they determine that BH feedback (specifically, their low-accretion, kinetic-feedback mode) plays a crucial role in setting the amount of Ovi in the CGM by affecting the amount of metal mass ejected by their galaxy.

We continue this ongoing investigation of the CGM using two sets of simulations: the cosmological volume, ROMULUS25 (Tremmel et al. 2017) and three "genetically modified" variations of an isolated, zoom-in Milky-Way (MW) mass galaxy (Roth et al. 2016; Pontzen et al. 2017a) simulated with and without the implementation of BH physics (Tremmel et al. 2015). We examine the effects of both environment and internal galaxy processes on the physical state and content of the CGM. Specifically, we address:

- How the star formation and accretion history of the galaxy co-evolve with the CGM.
- How SMBH activity imprints itself on the CGM.

First, we examine the CGM in a range of MW-mass galaxies with varied morphologies from ROMULUS25. Additionally, from a cosmological volume, we selected a Milky Way-analog based on halo mass for our zoom-in simulations. From this isolated MW-mass galaxy and its subsequent "genetic modifications", we quantify the effect of SMBH feedback on the CGM by examining a set of star forming and passive galaxies run both with and without BH physics. Using these isolated, zoom-in simulations in tandem with the Romulus25 simulation, we illuminate the roles that stellar evolution and SMBH feedback play in setting the properties of the CGM of MW-mass galaxies.

In Section 2, we describe the underlying physics used in our two galaxy samples. Section 3 details our results from examining the CGM in ROMULUS25 and comparisons with the zoom-in galaxies. We discuss these results and their implications for future studies in Section 4. In Section 5, we summarize our conclusions.

2. SIMULATION PARAMETERS

2.1. *ChaNGa Physics*

Both ROMULUS25 (hereafter R25) and our set of zoom-in galaxies were run using the smoothed particle hydrodynamics (SPH) N-body tree code, Charm N-body GrAvity solver (Menon et al. 2015, ChaNGa). ChaNGa includes the same models for a cosmic UV background, star formation (using a Kroup IMF), 'blastwave' SN feedback, and low temperature metal line cooling as previously used in GASOLINE (Wadsley et al. 2004, 2008; Stinson et al. 2006; Shen et al. 2010). ChaNGa includes an improved SPH formalism which includes a geometric density approach in the force expression. This update to the hydrodynamic treatment includes thermal diffusion (Shen et al. 2010) and reduces artificial surface tension allowing for better resolution of fluid instabilities (Ritchie & Thomas 2001; Menon et al. 2015; Governato et al. 2015).

Additional improvements have been made to the BH formation, accretion, and feedback models as well an improved prescription for dynamical friction (Tremmel et al. 2015, 2017). BH seed formation is tied to dense, extremely low metallicity gas to better estimate SMBH populations in a wide range of galaxies. Sub-grid models for both dynamical friction —to better simulate realistic SMBH dynamical evolution and mergers —and accretion have been implemented. The new SMBH accretion model considers angular momentum supported gas from nearby gas allowing for more physical growth compared to Bondi-Hoyle prescription alone or other methods that require additional assumptions or free parameters (Rosas-Guevara et al 2015, Anglés-Alcázar et al 2017). Angular momentum support is taken into account in the accretion equation:

$$\dot{M} \sim \frac{\pi (GM)^2 \rho c_s}{(v_{theta}^2 + c_s^2)^2} \tag{1}$$

where v_θ is the rotational velocity of the gas surrounding the BH and is informed by the angular momentum support of the gas on the smallest, resolvable scale. SMBH feedback energy is imparted on the nearest 32 particles gas particles according to a kernel probability and is determined by the accreted mass, $\dot{M}$, as:

$$E = \epsilon_r \epsilon_f \dot{M} c^2 dt, \tag{2}$$

where $\epsilon_r = 0.1$ and $\epsilon_f = 0.02$ are the radiative and feedback efficiency, respectively, and dt represents one black hole timestep, during which the accretion is assumed to be constant.

All our simulations were run with a ΛCDM cosmology from the most recent Planck collaboration utilizing $\Omega_m = 0.3086$, $\Omega_\Lambda = 0.6914$, h = 0.67, $\sigma_8 = 0.77$ and have Plummer equivalent force softening lengths of 250 pc. For simulating the cosmic reionization energy, both simulations enact a UV background at z ∼ 9 (Haardt & Madau 2012).

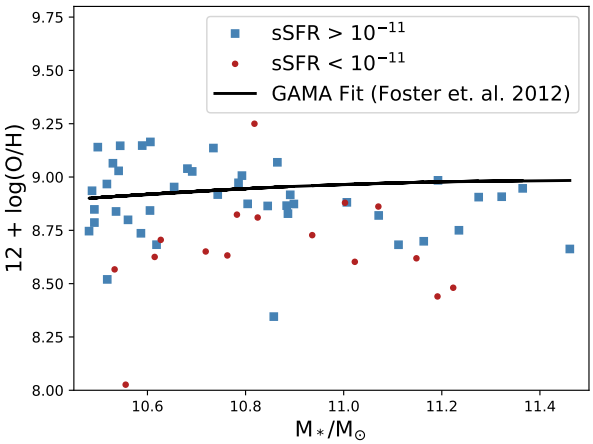

FIG. 1.— R25 is an SPH simulated cosmological volume with galaxy halos spanning the orders of 10^9 —10^{13} $M_\odot$. We show that the 58 galaxies in our sample fall well within the mass-metallicity relation. Red circles and blue squares represent passive and star forming galaxies, respectively. The solid black line shows the MMR fit from the Galaxy and Mass Assembly (GAMA) survey (Foster et al. 2012).

2.2. *Romulus 25 Cosmological Volume*

The ROMULUS25 (Tremmel et al. 2017, R25) simulation is a cosmological volume which includes galaxy halos within the mass range 10^9 —10^{13} $M_\odot$. R25 has a mass resolution of 3.4×10^5 $M_\odot$ and 2.1×10^5 $M_\odot$ for DM and gas particles, respectively. Galaxies in R25 have been shown to lie along the M-σ and SMHM relation, and are consistent with observations of star formation and SMBH accretion histories at high redshift (Tremmel et al. 2015). Additionally, Tremmel et al. (2015) shows that SMBH physics is a necessary component for reproducing the evolution of MW-mass galaxies as well as quenching in massive galaxies. For our study, we focus on the galaxies in R25 that fall within the stellar mass range of COS-Halos: 3×10^{10} $M_\odot$ and 3×10^{11} $M_\odot$. We examine all the galaxies within the specified mass range. With these selection criteria in place, our sample includes 58 (without excluding possible satellite galaxies). Using the sSFR cut of COS-Halos, 42 of these galaxies are star forming (sSFR $< 1.6 \times 10^{-11}$ $M_\odot$ yr^{-1}) and 16 are passive. We use the factor of 1.6 to account for the fact that COS-Halos uses a Sal-Peter IMF while our simulations use a Kroupa IMF (Kroupa et al. 1993). Figure 1 shows that the galaxies in our sample lie along the mass-metallicity relation (MMR). Red circles and blue squares represent passive and star forming galaxies, respectively. The solid black line shows the MMR fit from the Galaxy and Mass Assembly (GAMA) survey (Foster et al. 2012).

2.3. *Zoom-In Galaxies: Patient 0 and its Genetic Modifications*

While Romulus25 gives cosmological context to our analysis, we examine our set of genetically modified zoom-in galaxies to better understand the physical mechanisms at play. To select our galaxy, we ran initial uniform-volume, 50 h^{-1} Mpc on a side, dark matter-only cosmological volume. From this volume, we selected an isolated MW-mass ($M_{vir} \sim 10^{12}$) halo at z=0 as our "Patient 0" (hereafter P0) and then re-simulated it at a higher resolution with baryons. We additionally required that the galaxy be >2 Mpc away from another MW- or higher mass galaxy and selected it for the satellite galaxy contained within its virial radius at z = 0. For the subsequent, "genetically modified" (GM) zoom-in runs, we use the method of genetic modification of Pontzen et al. (2017a) which creates a set of very similar initial conditions that result in subsequent galaxy simulations which keep the large scale structure and cosmological conditions ΛCDM consistent (as in P0), while resulting in slight modifications to their accretion histories (Roth et al. 2016). For our purposes, we decreased the mass of the satellite which exists at z = 0 in P0 and shrank its mass *prior* to when it enter the galaxy at z = 1. To create the modified set of initial conditions, we determined which elements in the linear overdensity field of the initial condition grid map to the particles in the satellite. We then decreased the mean overdensity of these elements in the initial linear vector, all the while, maintaining the mean overdensity of the elements mapping to the main halo to preserve the final mass.

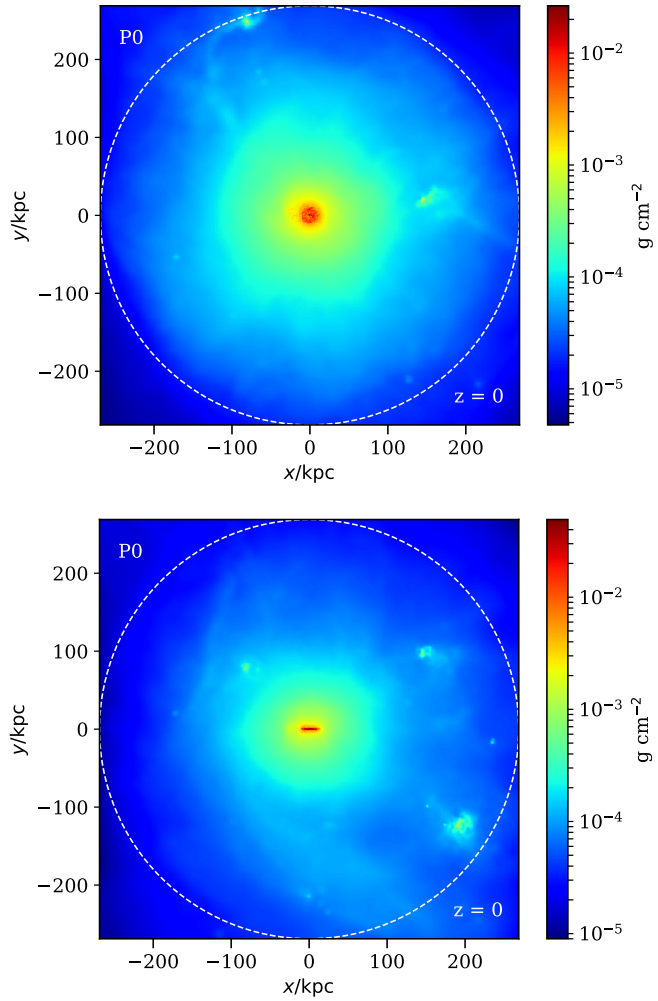

FIG. 2.— A face-on and edge on gas density image of our initial Milky Way-mass galaxy, Patient 0, at z = 0.

Patient 0 (and its 3 GM simulations) have a mass resolutions of 1.4×10^5 $M_\odot$ and 2.1×10^5 $M_\odot$ for DM and gas particles, respectively. The DM field in these galaxies is simulated at twice the gas linear resolution

to reduce noise in the potential near the galactic center (Pontzen et al. 2017a) and more accurately trace black hole dynamics (Tremmel et al. 2015).

2.3.1. *Galaxies with BH Physics*

TABLE 1
ZOOM-IN GALAXIES MODIFICATIONS **at z = 1**

Sim	Satellite Dark Matter Mass ($M_\odot$)
P0 & noBH	7.3×10^{10}
GM1 & noBH	5.9×10^{10}
GM2 & noBH	4.0×10^{10}
GM3 & noBH	2.5×10^{10}

At z = 0, our P0 galaxy is a star forming galaxy with a disk (Figure 3). P0 has an incoming satellite at z = 0 with an original mass of 7.34×10^{10} $M_\odot$ (mass ratio, q = 0.12) *prior* to entering the main halo's virial radius at z $\sim$ 1. For each GM galaxy simulation, we systematically shrink this satellite halo's mass prior to its entry with the main halo (Table 1). GM1 results in a similar disked, star forming galaxy as P0, while GM2 and GM3 become quenched at z $\sim$ 1 (Table 2).

While these GM galaxies are generated using the same method as Pontzen et al. (2017a), their study examines a different set of galaxies. The three galaxies in Pontzen et al. (2017a) were run to z = 2 and have $M_{Halo} \sim 10^{12}$. They each have incoming satellites whose masses are both increased and decreased prior to merging with the main galaxy, as in our galaxies; however, the resulting effect of their modifications were different from ours, as we explore in Section 2.3.3.

2.3.2. *Galaxies without BH Physics*

One key benefit of the individual zoom-in galaxies includes the ability to remove or adjust the physical parameters affecting our galaxies. This capability allows us to test different theoretical models which would be too computationally expensive to do with a large volume like R25. In particular, we may exploit this utility to understand directly the effects of the SMBH. To isolate the effect of the SMBH on the CGM, all four of the zoom-in simulations (P0 and its 3 GMs) were re-simulated at the same resolution and with all the same physics *excluding* BH formation, feedback, and dynamical friction (Table 3). Black hole seed formation was disabled and the BH feedback and accretion efficiency parameters were set to 0.

2.3.3. *Quenching in GM2 and GM3*

Pontzen et al. (2017b) previously explored the relationship between BH feedback and mergers and its effect on quenching, using the same genetic modification technique as we use for the GM galaxies in our study. They determine that SMBH feedback is critical to quenching a galaxy, which is consistent with our finding that the *only* quenched galaxies are in simulations that include SMBHs (Figure 3). Pontzen et al. (2017b) argues that the merger can disrupt the cold disk of the galaxy, which then allows the feedback of the SMBH to have a farther reaching effect on the star forming gas of the disk

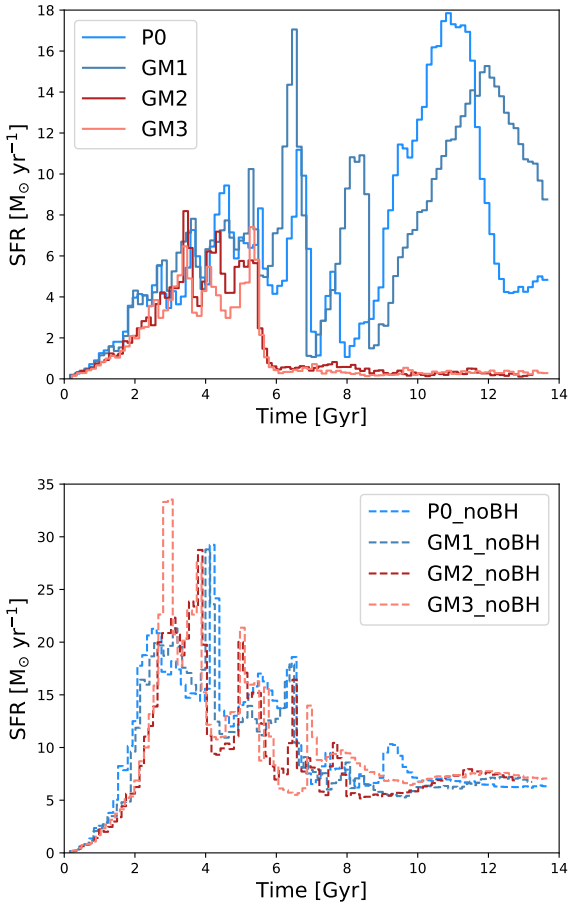

FIG. 3.— The star formation histories for the zoom-in galaxies: Patient 0 and its 3 GM galaxies with BH physics (*Upper*) and *Lower* without BH physics. In the galaxies including BH physics, P0 and GM1 remain star forming throughout their histories while GM2 and GM3 become quenched at z $\sim$ 1. Without BH physics, all four galaxies remain star forming until z = 0. This is an effect we will explore in future work.

thereby keeping the galaxy in a state of quiescence. The top panel of Figure 3 shows star formation histories of the four zoom-in galaxies with BH physics included. It demonstrates that, unlike P0 and GM1 which remain star forming throughout their history, GM2 and GM3 become quenched at z $\sim$ 1. This immediate quenching just after the merger of the satellite with the main halo *does not* take place in the set of zoom-in galaxies without BH physics, as predicted by Pontzen et al. (2017b). Contrastingly, the lower panel of Figure 3 shows the star formation histories of the four zoom-in galaxies without BH physics and all four of their histories remain star forming and are fairly similar. The stark differences between the GM2 and GM3 galaxies with and without BHs imply that some interplay between the satellite's mass and the SMBH feedback must play a pivotal role in quenching these galaxies so thoroughly.

We further examine the effects of the BH by looking to the accreted mass and accretion rates of the BHs. The upper panel in Figure 4a shows the cumulative accreted SMBH mass as a function of time. Here we see that the accreted mass growth in the quenched galaxies, GM2 and GM3, isn't significantly different than that of the star

TABLE 2
ZOOM-IN GALAXIES PROPERTIES *with BHs* AT **z = 0.17**

Sim	Total Halo Mass ($M_\odot$)	Total Gas Mass ($M_\odot$)	Total Stellar Mass ($M_\odot$)	CGM Gas Mass ($M_\odot$)	R_{vir} (kpc)	T_{vir} (K)
P0	9.9×10^{11}	1.1×10^{11}	5.0×10^{10}	9.3×10^{10}	277.0	5.5×10^5
GM1	9.7×10^{11}	9.9×10^{10}	4.7×10^{10}	8.5×10^{10}	274.9	5.4×10^5
GM2	8.1×10^{11}	6.9×10^{10}	1.4×10^{10}	6.9×10^{10}	259.2	4.8×10^5
GM3	6.6×10^{11}	5.1×10^{10}	1.1×10^{10}	5.1×10^{10}	241.7	4.2×10^5

TABLE 3
ZOOM-IN GALAXIES PROPERTIES *without BHs* AT **z = 0.17**; NEEDS UPDATING FOR NEW NOBH RUNS

Sim	Total Halo Mass ($M_\odot$)	Total Gas Mass ($M_\odot$)	Total Stellar Mass ($M_\odot$)	CGM Gas Mass ($M_\odot$)	R_{vir} (kpc)	T_{vir} (K)
P0noBH	9.8×10^{11}	8.2×10^{10}	7.9×10^{10}	7.5×10^{10}	276.1	5.4×10^5
GM1noBH	9.9×10^{11}	8.7×10^{10}	7.4×10^{10}	8.0×10^{10}	276.2	5.5×10^5
GM2noBH	9.6×10^{11}	8.8×10^{10}	7.0×10^{10}	8.0×10^{10}	274.0	5.3×10^5
GM3noBH	8.4×10^{11}	7.1×10^{10}	7.3×10^{10}	6.4×10^{10}	261.9	4.9×10^5

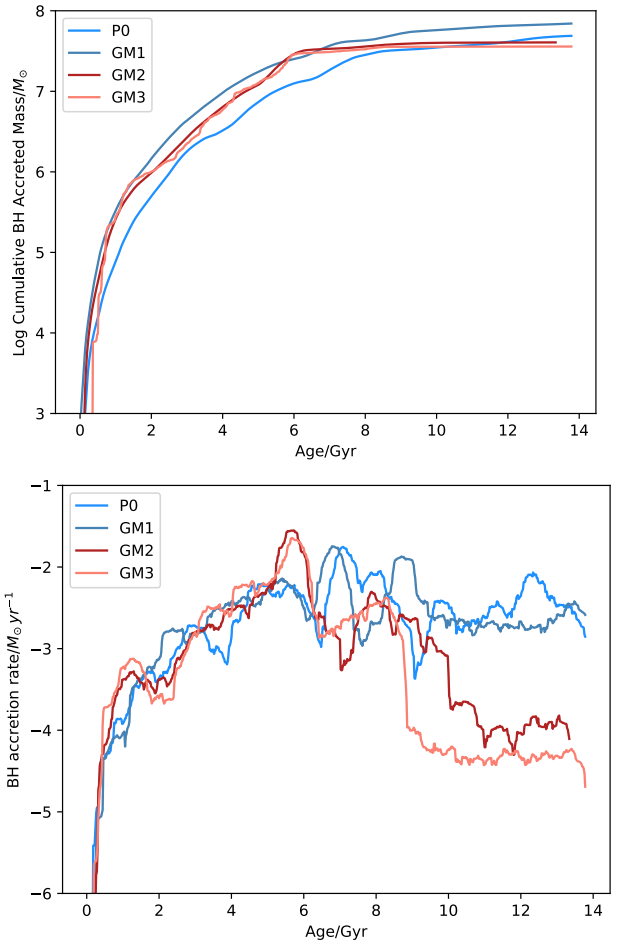

FIG. 4.— SMBH mass (*Upper*) and SMBH accretion rates (*Lower*) for our 4 zoom-in galaxies. Colors as in Figure 6. The SMBH growth of GM2 and GM3 occurs quicker than the growth of the SMBH in the two star forming zoom-in galaxies. In particular, GM3, which has the most significant modification to its satellite's mass, has a SMBH that grows quickest. Both quenched galaxies also have a sharp peak in accretion rate around the time of the merger with the satellite (z ∼ 1, t ∼ 6 Gyr), indicated by the dashed grey line.

forming galaxies. However, more significant differences arise in Figure 4b which depicts the SMBH accretion rates as a function of time. From this figure, we can see an increase of accretion occurs for both quenched galaxies near the time of the merger (z ∼ 1, t ∼ 6 Gyr). Though the BH's activity and growth are not directly affected by the changing mass of the incoming satellite, together the modified satellite mass and effect of the BH make a significant impact on the star formation history of the galaxy.

We note that the genetic modifications performed on the galaxies of (Pontzen et al. 2017a) was different from the ones implemented here. In their case, it was an increase of the satellite's mass that resulted in a quenched galaxy, rather than a shrinking as we implement here; however, due to the lower mass satellite in our case, we see that the mass is compensated by faster, early accretion (Figure 4).

This set of galaxies, which were produced from very similar initial conditions but which illustrate very different star formation and accretion histories, allows us to directly examine how assembly history may imprint itself on the CGM. Additionally, they allow us to concretely confirm the results of Pontzen et al. (2017b) that the effect of a SMBH, while not the only requisite, is *vital* to the quenching process in galaxies.

3. RESULTS

Individual halos in the ROMULUS25 cosmological volume and in the individual zoom-in galaxies are extracted using the Amiga Halo Finder (AHF) (Knollmann & Knebe 2009) and central SMBH positions and velocities are defined relative to the center position and inner 1 kpc center-of-mass velocity of their host halo, respectively. All zoom-in galaxies with BH physics are isolated with their most major merger occuring at z ∼ 1 (mass ratio = M_{halo}/M_{sat}, q <10) and their modified satellite halo still present at z = 0. The galaxies without BH physics have mergers at z = 1 and additional mergers [need to finish examining these simulations.]

The CGM of each individual galaxy halo (within the R25 galaxies and our zoom-ins) is defined as the mass en-

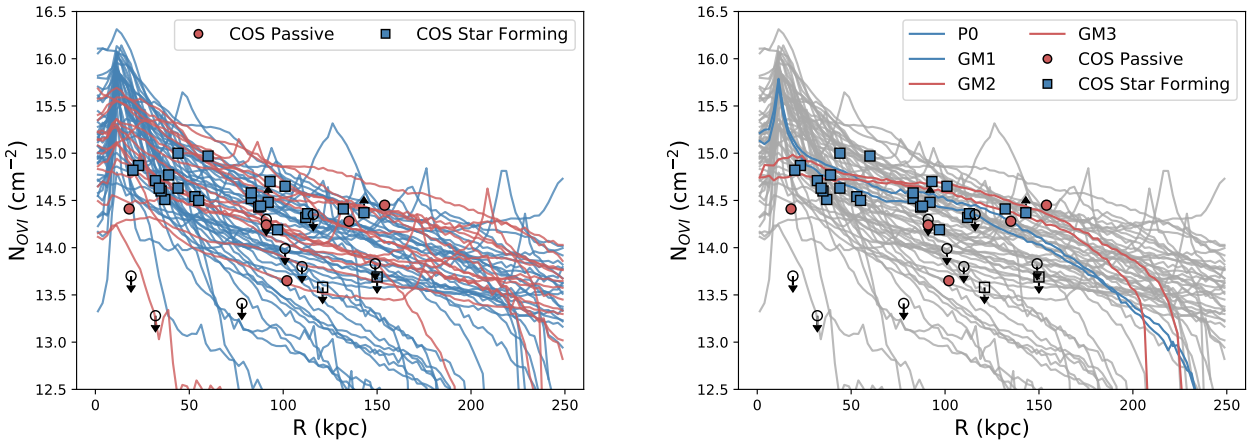

FIG. 5.— *Left:* Mean column densities of Ovi as a function of radius for all COS-Halo mass halos in the R25 simulation at z = 0.17. Blue and red lines distinguish between disk dominated spirals and quenched elliptical galaxies within the R25 simulation. *Right:* Column densities of Ovi in our family of zoom-in galaxies. Grey lines indicate R25 MW galaxy column densities from *Left*. Blue solid lines describe our two star forming galaxies, P0 and GM1. GM4-7, our passive galaxies, are in solid red. Filled circles and squares indicate spirals and ellipticals from the COS-Halos Survey dataset. Unfilled squares indicate upper limits.

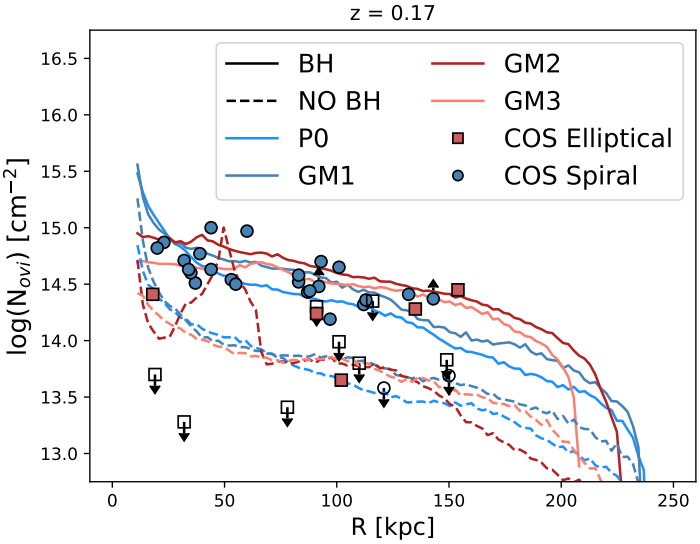

FIG. 6.— Column density profiles of Ovi in our 4 zoom-in galaxies with (solid lines) and without (dashed lines) BH physics. P0 and GM1, our two star forming galaxies are colored as light blue and dark blue, respectively. Our quenched galaxies, GM2 and GM3, are labeled in dark red and pink, respectively. These column densities show that the BH is essential to shaping the OVI in the CGM of star forming and passive galaxies alike.

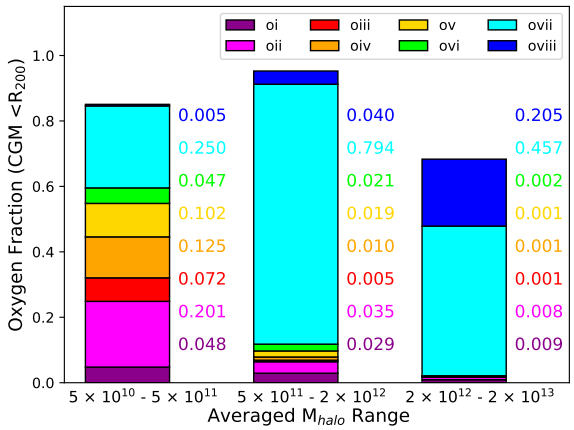

FIG. 7.— Oxygen ion fractions in the CGM of our 25 MW-mass galaxies and 11 high mass galaxies from R25. Log M_{Halo} for each halo are labeled in white text.

closed in an annulus from 10 kpc from the center position out to a virial radius defined as the radius at which the density is 200 times the critical density, ρ_c, where ρ/ρ_c = 200. While the genetic modification process results in galaxies with similar final masses, we find that the mass of the CGM correlates with the mass of the halo. P0, which results in the most massive halo at z ∼ 0, has the most mass in its CGM, while GM3 results in the least massive CGM mass and halo mass (Table 3).

3.1. *Ovi as a Tracer for Virial Temperature*

Column densities of Ovi are calculated using the analysis software Pynbody (Pontzen et. al. 2013). Oxygen enrichment from supernovae and winds is traced throughout the integration of the simulation and ionization states are calculated during post-processing, assuming optically thin conditions, a Haardt & Madau (2012) ultraviolet radiation field at z = 0, and collisional ionization equilibrium. Recent papers have raised concerns that this UV background is too weak (Kollmeier et al. 2014; Shull et al. 2015); however, as the Ovi in our simulations is predominantly collisionally ionized, our choice of UV background does not affect our results. We use the CLOUDY software package (Stinson et al. 2012; Ferland et al. 2013) to create models with varying temperature, density, and redshift to determine Ovi fractions for all the gas in each simulated galaxy. Figure 5a shows the column densities of Ovi as a function of radius for our 58 R25 MW-mass galaxies. Red and blue lines describe quenched and star forming galaxies within the sample, respectively. The COS-Halos dataset is plotted on top in black, with squares and circles distinguishing between elliptical and spiral galaxies. Upper and lower limits are designated with arrows and unfilled markers. The R25 galaxies well match the observations from the COS-Halos

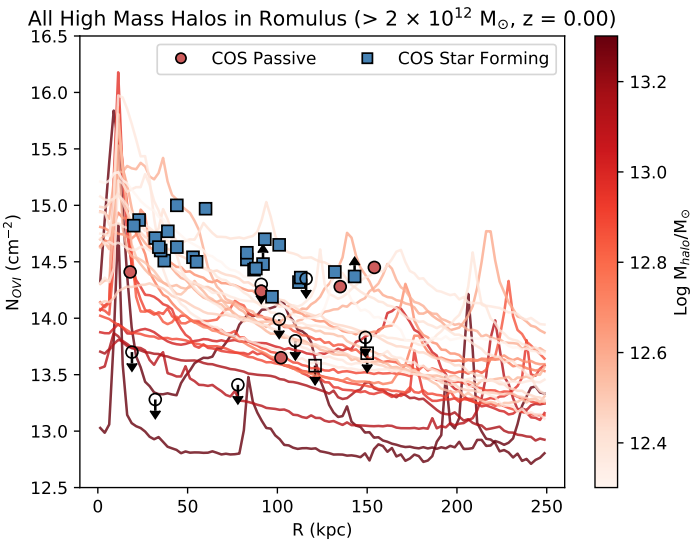

FIG. 8.— Column density profiles of Ovi in the high mass galaxies of R25.

Survey. We further compare the column densities of Ovi in the R25 galaxies to the 4 zoom-in galaxies with BH physics and find that these galaxies also well match the observed column densities of COS-Halos and fall within the range of the R25 galaxies (Figure 5b).

Figures 5 and 6 make it clear that our simulations reproduce the column densities of Ovi in the CGM. In addition, we note that *the column densities of Ovi in the CGMs of these galaxies does not depend on the assembly history of the galaxy.* We see this in both R25, which in addition to providing evidence for this initial result also gives cosmological credence to our suite of GM galaxies, and our four GM galaxies that include BH physics. We confirm our result with Patient 0 and its GMs, which include two star forming galaxies and two quenched galaxies, all of which well match the Ovi observations despite differing assembly histories. (Figure 6)

Figure 7 shows the average ionization fractions for all the ionization states of oxygen within three mass ranges: low mass (5×10^{10} —5×10^{11} $M_\odot$), Milky Way-mass (5×10^{11} —2×10^{12} $M_\odot$), and high mass (2×10^{12} —2×10^{13} $M_\odot$). The Ovi fractions decrease from the MW-mass range to the high mass regime due to the increase in virial temperature which moves from a value close to the ionization peak for Ovi, T $\sim 10^{5.5} K$ to $10^{6.3}$ K. Similarly, Figure 8 confirms that as galaxy virial mass increases, column densities of Ovi decrease. From this study, we determine that morphological evolution of the galaxy doesn't correlate with the evolution of Ovi in the CGM. Instead, it appears that the mass of the galaxy, as traced by its virial temperature [Table 2], plays a more significant role in determining the column density of Ovi seen in the CGM.

3.2. *Metal Transport by the SMBH*

We examine the column densities of Ovi in the CGMs of our 4 zoom-in galaxies *without* BH physics and compare them to the cases where BH physics is included. Figure 6 shows the column densities of Ovi in the CGM of all four of our zoom-in galaxies with BH physics (solid lines) and without (dashed lines). We can see that in the cases where BH physics is not included, the values of N_{Ovi} are significantly lower implying that the presence of the SMBH must play an important role in populating Ovi in the CGM. We look to the temperature, mass, density, and metallicity of the CGM to investigate the cause of this decrease in Ovi. (Figure 9)

The difference between the CGMs of these two cases appears to come directly from the change in metallicity due to the lack of black hole activity. (Figure 9) We examine the metallicity of the disk to look for further clues about how the lack of SMBH activity is affecting the galaxy. Figure 10 shows that, in the galaxies without BH physics, the metals produced in the disk aren't driven into the CGM due to the lack of SMBH feedback. This result is consistent with what we see in Figure 12. The lack of high metallicity gas in the CGM phase diagrams of the galaxies with no BH physics (*Right Column*) confirms the fact that metals are not being driven out of the disk. We find that feedback does not play a significant role in heating or excavating the CGM gas, but instead the SMBH's feedback is pivotal in *transporting the metals* from the center of the galaxy out into the CGM. *The SMBH plays a significant role in physically driving the metals out of the disk and into the outer regions of the CGM.*

[Include discussion about metal flux into and out of galaxy (once complete); comparisons between observations and amount of total metals in disk (plus metal gradients)]

3.3. *Qualitative CGM Properties*

Figure 11 shows the phase diagrams of the CGMs of the 4 zoom-in galaxies both with and without BH physics. Examining the CGM phase diagrams for the GMs that include BH physics (*Left Column*), we note the following key differences: less overall mass from the uppermost (P0) to lowermost (GM3) figure; variations in the amount of cool, dense gas (T $<10^{4.5}$, n_H $>10^{-3}$); and the lack of hot, dense gas (T $>10^{5.5}$, n_H $>10^{-3}$) in the phase diagrams of GM2 and GM3, our quenched galaxies. Examining the CGM phase diagrams that *exclude* BH physics (*Right Column*), we don't see any significant differences.

There is a lack of the hot, dense gas in the quenched galaxies that is present in the star forming galaxies, P0 and GM1. We note that this feature is also present in the CGM diagrams of the galaxies *without* BH physics, which all result in star forming, disked galaxies. Figure 12 further examines this difference with the same CGM phase diagrams of P0 and GM2 colored by mass, metallicity, and distance from the center of the galaxy, with (*Two Upper Rows*) and without (*Two Lower Rows*) BH physics. The hot, dense gas in P0 with BH physics (*Upper Row*) appears to be mostly comprised of high metallicity gas that is close to the disk (R <50 kpc). Further examining this gas, we find that 3 % of the CGM gas has metallicity Z $>Z_\odot$ at z = 0.17. Furthermore, of this 3 %, nearly 30 % is farther than 20 kpc from the center of the galaxies. For GM1, the CGM is comprised of 6.7 % gas with Z $>Z_\odot$ with 55 % of that gas farther than 20 kpc. Contrastingly, a negligible amount of the CGM of both GM2 and GM3 have Z $>Z_\odot$ at z = 0.17. The CGMs

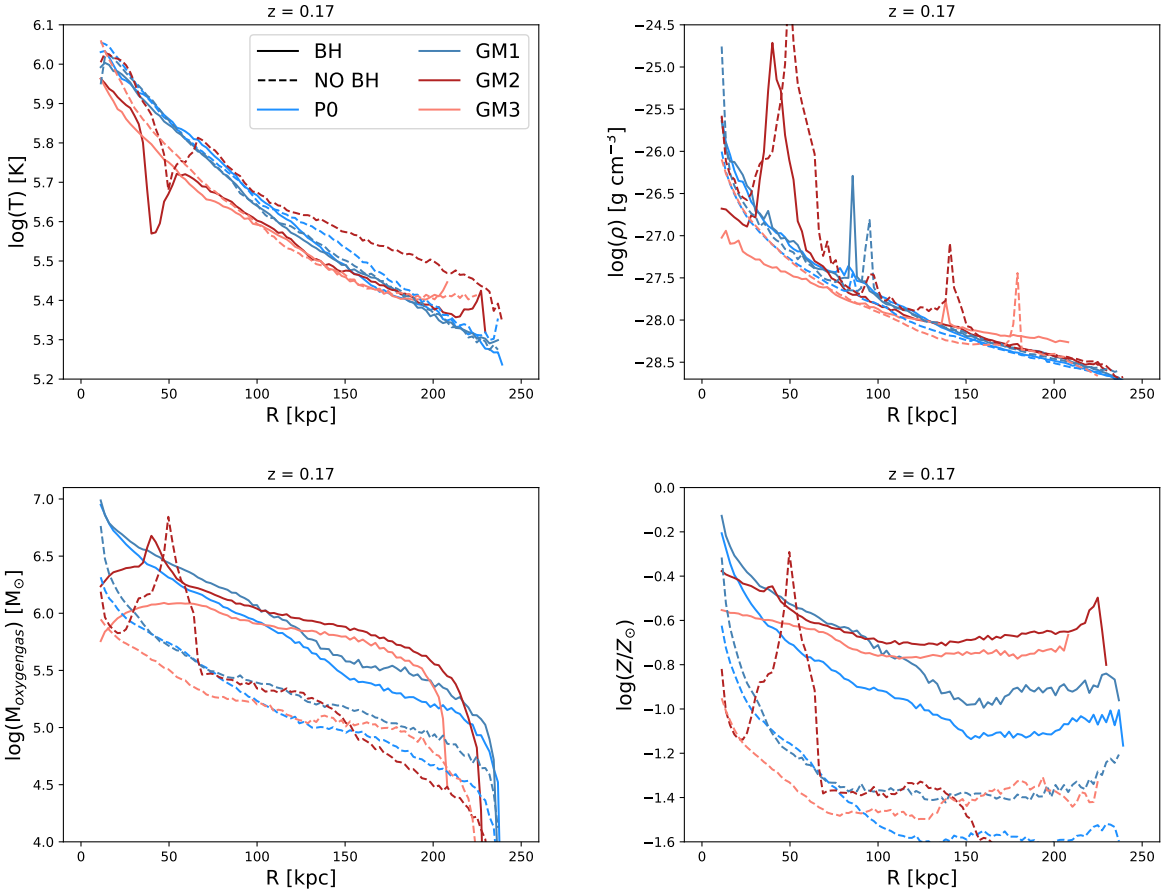

FIG. 9.— Temperature, Total Mass, Total Density, and Metallicity profiles of the CGM of our 4 zoom-in galaxies with and without BH physics. Colors and linestyles as in Figure 6.

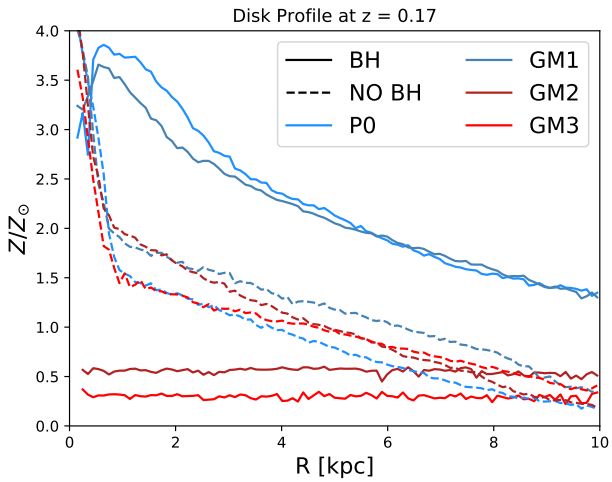

FIG. 10.— Metallicity profile of the gas within the disk of our 4 zoom-in galaxies with and without BH physics. Colors and line styles as in Figure 9. Without the black hole physics, metals remain trapped near the center of the disk with no mechanism to propagate out into the CGM.

of the four galaxies without BH physics also have small amounts of gas with Z $>$Z$_\odot$, from 0.1 % in P0noBH to 0.04 % in GM3noBH. These percentages of high metallicity gases in P0 and GM1 with BH physics point to metal exchange in the galaxy that is strongly dependent on the SMBH (which we discuss further in Section 3.2). The removal of the BH physics in all four zoom-ins results in 4 galaxies with incredibly similar properties by z = 0.17 (Table 3). Though they are significantly different than their counterparts with BH physics, all 4 of the galaxies without BH physics have phase diagrams that are quite similar to each other indicating that the BH plays a strong role in shaping the CGM in these galaxies. This difference between the galaxies with and without BH physics is also visible in the column densities of Ovi, which we explore below.

4. DISCUSSION

Limitations of the simulations
Comparisons with other groups: Nelson, Suresh, Oppenheimer, Ford
BH/CGM observation predictions
- Including plots of BH mass vs Novi at 75 kpc

5. CONCLUSION

Result 1: Ovi as a Tracer for Virial Temperature of the Halo

The combined, consistent results of the cosmological R25 and our 4 zoom-in galaxies (which include BH physics) imply a mechanism by which column densities of Ovi are set by the virial temperature of the CGMs host galaxy. They aren't affected by the evolution of a disk. Their phase diagrams also show significant difference in response to their overall assembly history, showing more,

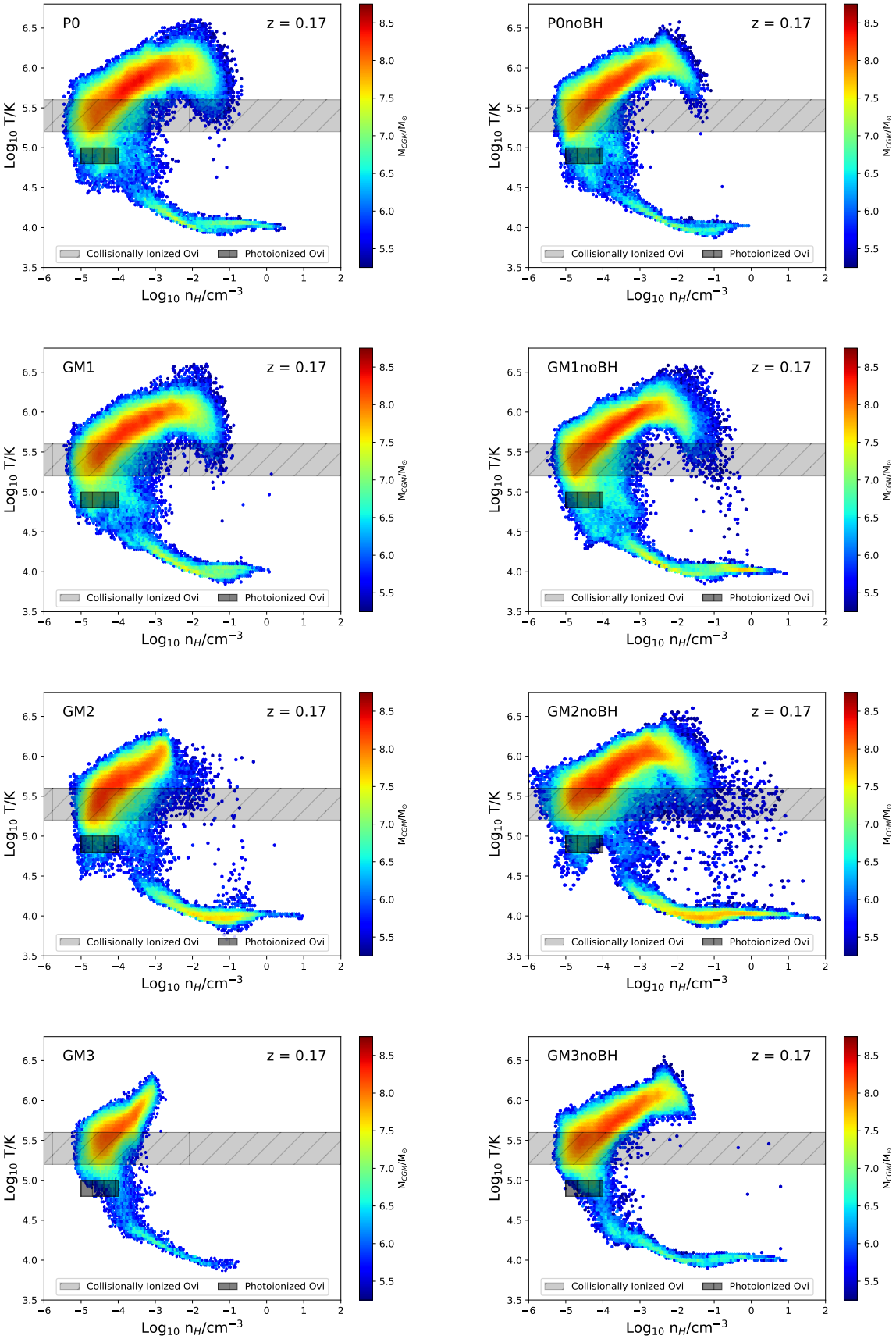

FIG. 11.— Phase diagrams of the temperature and density of the two star forming zoom-in galaxies, P0 (*Top row*) and GM1 (*Second row*), and the two quenched galaxies, GM2 (*Third row*) and GM3 (*Bottom row*). The phase diagrams of galaxies with BH hole physics vary quite widely between the star forming (P0 and GM1) and quenched cases (GM2 and GM3), particularly in the highest temperature and density gas. However, the phase diagrams of the galaxies without BH physics appear nearly identical, as are their star formation histories.

higher metallicity gas in the star forming cases. Nevertheless, the column densities of Ovi remain consistent despite differences in star formation history and the significant variations of their phase diagrams. Therefore, we surmise that the differences in the CGM are not determined by whether or not a galaxy quenches but rather the conditions for Ovi are primarily set by the amount of metals propogated into the disk by the BH and the virial temperature of the galaxy.

These results are consistent with those of Oppenheimer et. al. 2016 who used a suite of EAGLE simulated galaxies to examine the bimodality of Ovi column densities (further discussed in [Tumlinson 2011]) in star forming and quenched galaxies. They argue that the star forming galaxies (M_{halo} = 10^{11} - 10^{12} $M_{\odot}$), which were found to have a higher fraction of Ovi, were at the right virial temperature to maximize Ovi production, while their quenched galaxies (M_{halo} = 10^{12} - 10^{13} $M_{\odot}$) had high enough virial temperatures such that the dominant ionization state was not Ovi but rather OviI or above. Oppenheimer et. al. 2016 argues that the Ovi content was not a tracer of star formation directly, but rather a more direct thermometer for the temperature of the halo.

We note that the quenched galaxies in our sample have slightly smaller halo masses than our star forming galaxies, unlike those in Oppenheimer, explaining the lack of bimodality that we observe. While all the GMs are in the mass range to have virial temperatures which optimize Ovi, we further examine the R25 simulation's higher mass, passive galaxies in addition to the MW-mass galaxies (which have virial temperatures spanning 5.8 $\times$ 10^5 K —1.1 $\times$ 10^6 K) to see if the bimodality appears. (Figure 7) We determine that the Ovi still prOvides a direct thermometer for the temperature of the halo.

Furthermore, examining galaxies with masses larger than our MW-mass GMs (>2 $\times$ 10^{12}) from the R25 suite, we see that the column densities of Ovi decrease as the ionization peak of Ovi is surpassed by these halos. Since the virial temperature is higher, the oxygen is likely to be ionized to a higher ionizations state (OviI or OviI), which we show is the case in Figure 7.

Result 2: SMBH as driver for metals in the CGM

Our result that the SMBH acts a physical driver for metals in the CGM has surprising consequences. Previous studies have examined the effect of heating on the CGM as the SMBHs energy input may put the gas into phases which optimize the production of Ovi. (Suresh et al. 2017) Others have proposed that the feedback from SMBH may physically drive outflows of gas out of the galaxy, resulting in a lower density CGM and therefore lower densities of Ovi. Neither of these cases are what we see. *Instead, we see a suite of CGM which rely on the SMBH for the propagation of metal mass (but not total gas mass) into the outer galaxy and Ovi columns which depend on the virial temperature of the galaxy.* (Figure 10)

Acknowledgements

REFERENCES

Cen, R. 2013, Astrophysical Journal, 770, 1 1

Ferland, G. J., Porter, R. L., Van Hoof, P. A. M., et al. 2013, Revista Mexicana de Astronomia y Astrofisica, 49, 137 3.1

Ferrarese, L., & Merritt, D. 2000, The Astrophysical Journal, 539, L9 1

Ford, A. B., Werk, J. K., Davé, R., et al. 2016a, Monthly Notices of the Royal Astronomical Society, 459, 1745 1

—. 2016b, Monthly Notices of the Royal Astronomical Society, 459, 1745 1

Foster, C., Hopkins, A. M., Gunawardhana, M., et al. 2012, 1 1, 2.2

Gebhardt, K., Kormendy, J., Ho, L. C., et al. 2000, The Astrophysical Journal, 543, L5 1

Governato, F., Weisz, D., Pontzen, A., et al. 2015, Monthly Notices of the Royal Astronomical Society, 448, 792 2.1

Haardt, F., & Madau, P. 2012, The Astrophysical Journal, 746, 125 2.1, 3.1

Knollmann, S. R., & Knebe, A. 2009, The Astrophysical Journal Supplement Series, 182, 608 3

Kollmeier, J. A., Weinberg, D. H., Oppenheimer, B. D., et al. 2014, The Astrophysical Journal, 789, L32 3.1

Kormendy, J., & Ho, L. C. 2013, Annual Review of Astronomy and Astrophysics, 51, 511 1

Kroupa, P., Tout, C. A., & Gilmore, G. 1993, Monthly Notices of the Royal Astronomical Society, 262, 545 2.2

Mcconnell, N. J., & Ma, C.-P. 2013, The Astrophysical Journal, 764, 184 1

Menon, H., Wesolowski, L., Zheng, G., et al. 2015, Computational Astrophysics and Cosmology, 2, 1 2.1

Nelson, D., Kauffmann, G., Pillepich, A., et al. 2018, Monthly Notices of the Royal Astronomical Society, 477, 450 1

Oppenheimer, B. D., & Davé, R. 2008, Monthly Notices of the Royal Astronomical Society, 387, 577 1

Oppenheimer, B. D., Crain, R. A., Schaye, J., et al. 2016, Monthly Notices of the Royal Astronomical Society, 460, 2157 1

Pontzen, A., Tremmel, M., Roth, N., et al. 2017a, Monthly Notices of the Royal Astronomical Society, 465, 547 1, 2.3, 2.3.1, 2.3.3

—. 2017b, Monthly Notices of the Royal Astronomical Society, 465, 547 2.3.3

Reines, A. E., & Volonteri, M. 2015, The Astrophysical Journal, 813, 82 1

Ritchie, B. W., & Thomas, P. A. 2001, Monthly Notices of the Royal Astronomical Society, 323, 743 2.1

Roth, N., Pontzen, A., & Peiris, H. V. 2016, Monthly Notices of the Royal Astronomical Society, 455, 974 1, 2.3

Shen, S., Wadsley, J., & Stinson, G. 2010, Monthly Notices of the Royal Astronomical Society, 407, 1581 2.1

Shull, J. M., Moloney, J., Danforth, C. W., & Tilton, E. M. 2015, Astrophysical Journal, 811, 3 3.1

Springel, V., & Hernquist, L. 2005, The Astrophysical Journal, 622, L9 1

Stinson, G., Seth, A., Katz, N., et al. 2006, Monthly Notices of the Royal Astronomical Society, 373, 1074 2.1

Stinson, G. S., Brook, C., Prochaska, J. X., et al. 2012, Monthly Notices of the Royal Astronomical Society, 425, 1270 3.1

Suresh, J., Rubin, K. H. R., Kannan, R., et al. 2017, Monthly Notices of the Royal Astronomical Society, 465, 2966 1, 5

Tremmel, M., Governato, F., Volonteri, M., & Quinn, T. R. 2015, Monthly Notices of the Royal Astronomical Society, 451, 1868 1, 2.1, 2.2, 2.3

Tremmel, M., Karcher, M., Governato, F., et al. 2017, Monthly Notices of the Royal Astronomical Society, 470, 1121 (document), 1, 2.1, 2.2

Tumlinson, J., Peeples, M. S., & Werk, J. K. 2017, Annual Review of Astronomy and Astrophysics, 55, 389 1

Tumlinson, J., Thom, C., Werk, J. K., et al. 2011, Science, 334, 948 1

Volonteri, M., & Bellovary, J. 2012, Reports on Progress in Physics, 75, 1 1

Wadsley, J., Stadel, J., & Quinn, T. 2004, New Astronomy, 9, 137 2.1

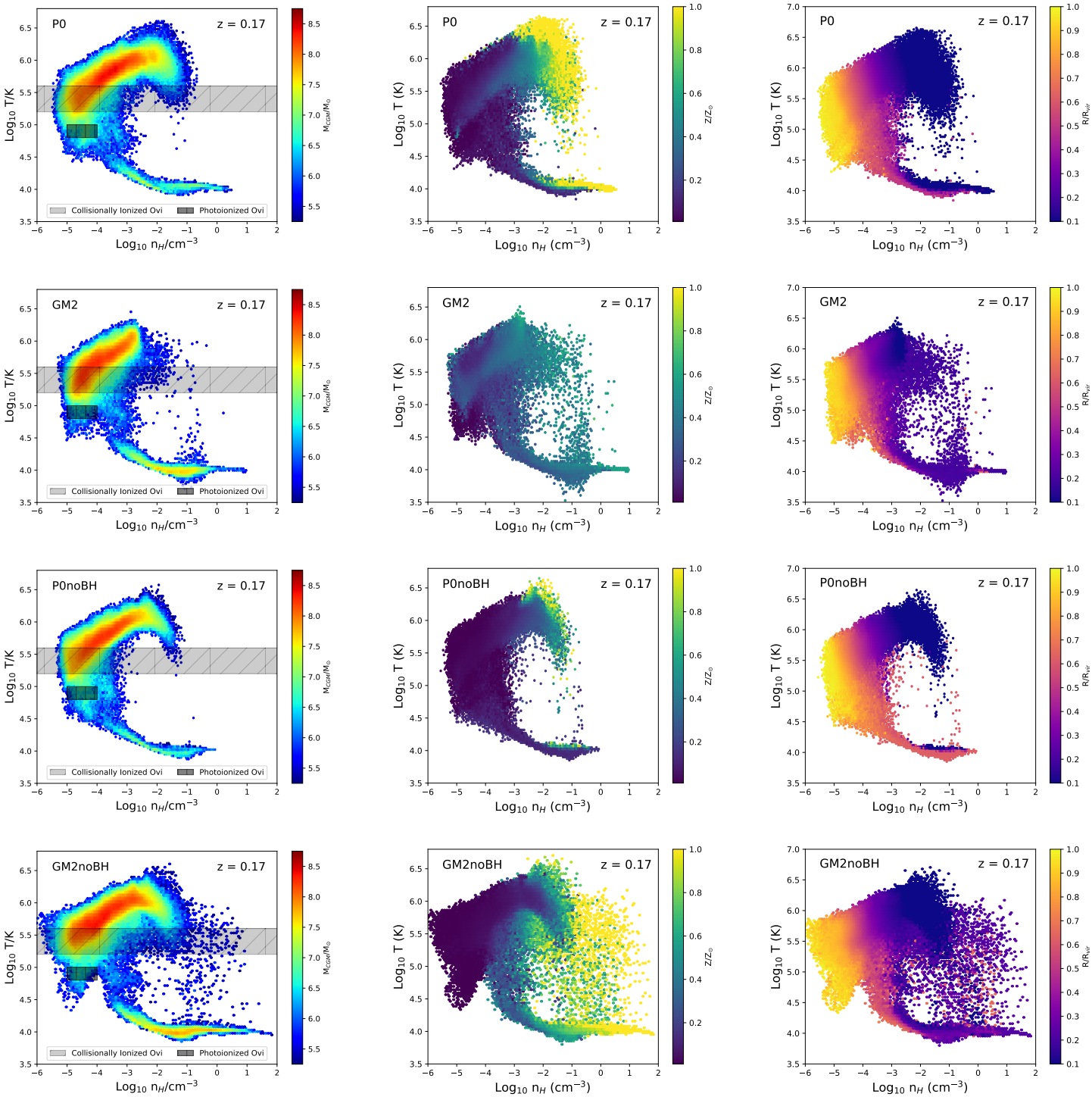

FIG. 12.— Phase diagrams of the temperature and density of the star forming zoom-in galaxy, P0 (*Top row* with BH physics, *Middle row* without), and the quenched galaxy, GM2 (*Bottom row*). *Left:* The phase diagrams of galaxies with BH hole physics show stark differences between the star forming (P0 and GM1) and quenched cases (GM2 and GM3). particularly in the highest temperature and density gas. *Middle:* The same phase diagram showing temperature and density, however, the colorbar is weighted by the average metallicity of the star in each bin. We note that the high density, high temperature gas we see in the star forming P0, is also the highest metallicity gas in the CGM. *Right:* Similarly, a phase diagram with the colorbar now weighted by the average distance from the center of the galaxy of the gas particles in each bin.

Wadsley, J. W., Veeravalli, G., & Couchman, H. M. P. 2008, Monthly Notices of the Royal Astronomical Society, 387, 427 2.1
Werk, J. K., Prochaska, J. X., Thom, C., et al. 2012, The Astrophysical Journal Supplement Series, 198, 3 1
—. 2013, The Astrophysical Journal Supplement Series, 204, 17 1
Werk, J. K., Prochaska, J. X., Tumlinson, J., et al. 2014, The Astrophysical Journal, 792, 8 1
Werk, J. K., Prochaska, J. X., Cantalupo, S., et al. 2016, 24 1